

## Coupling between two ferromagnetic layers separated by an antiferromagnetic layer

Haiwen Xi and Robert M. White

*Data Storage Systems Center, Carnegie Mellon University, Pittsburgh, Pennsylvania 15213*

(Received 11 February 2000)

We have investigated the interlayer exchange coupling between two ferromagnetic (FM) layers mediated by an antiferromagnetic (AF) layer. We have extended Slonczewski's "proximity magnetism" idea in the trilayers by including an AF magnetocrystalline anisotropy and considering interfacial exchange coupling that is influenced by the interface roughness. Using a continuum model we obtain the rotation behavior of the AF moments during FM magnetization reversal. The results are discussed within the context of the "proximity magnetism" model. The FM magnetization behavior and the interlayer coupling are strongly dependent on the interfacial exchange coupling and the AF thickness, compared with the AF domain wall energy  $\sigma_w$  and the wall length  $\delta_w$ , respectively. A study of the exchange anisotropy in FM/AF bilayers is also presented.

### I. INTRODUCTION

A considerable amount of research on magnetic thin films has been stimulated since the original discovery of the giant magnetoresistive (GMR) effect in magnetic multilayers.<sup>1</sup> The GMR effect is currently being used by the data and information storage industry in recording heads and for magnetic random access memories (MRAM) as part of a spin valve structure.<sup>2</sup> A typical spin valve consists of two ferromagnetic (FM) layers separated by a nonmagnetic (NM) layer.<sup>3</sup> One FM layer is expected to rotate freely. The other is pinned by an antiferromagnetic (AF) layer utilizing the exchange bias effect, which was discovered more than 40 years ago.<sup>4</sup> To optimize the spin valve design, one must consider the interlayer exchange coupling between the two FM layers as well as the FM/AF exchange coupling (exchange bias) of the pinned layer.

Both aspects of such a trilayer have been the subjects of extensive investigations and are still under study. The exchange bias effect is so named because the phenomena manifests itself in a shifted hysteresis loop for a FM in contact with an AF as a result of interfacial exchange coupling.<sup>4,5</sup> Recently, we have investigated the behavior of a FM/AF bilayer by extending the work of Néel<sup>6</sup> and Mauri *et al.*<sup>7</sup> to take into account the twisting of the AF moments as the FM magnetization is rotated.<sup>8</sup> Based on this model, we were able to describe the reversible and irreversible behavior of the AF, clarify the origin of the exchange bias, the enhanced coercivity, and the hysteresis energy loss,<sup>9</sup> and concluded that the exchange anisotropy can not exceed the domain wall energy of the AF.<sup>8</sup> Furthermore, a plausible explanation of was given of the recent observation that the value of exchange anisotropy deduced from hysteresis measurements differs from that deduced, for example, from ac susceptibility measurements and ferromagnetic resonance measurements.<sup>10</sup> More recently, we have also applied a similar approach<sup>11</sup> to investigate FM/AF bilayers with a "spin flop" configuration, which has been observed in some FM/AF systems,<sup>12</sup> and has been theoretically discussed first by Koon<sup>13</sup> and later by Schulthess and Butler.<sup>14</sup>

In this paper we have extended our approach to consider a FM/AF/FM trilayer system. In such a system the FM layers

experience an oscillatory exchange coupling and occasionally a biquadratic (nonlinear) exchange coupling as well.<sup>15</sup> Since the interfaces of the layers in a multilayer structure are not smooth, Slonczewski<sup>16</sup> first proposed a mechanism for biquadratic coupling which results from the frustration of the bilinear coupling associated with the surface roughness. Later, Slonczewski suggested another coupling mechanism for multilayers with Cr or Mn as the interlayer based on their antiferromagnet nature.<sup>17</sup> In this so-called "proximity magnetism model," the short-range exchange coupling in the bulk of AF interlayer and the exchange coupling across the interfaces are taken into account. A perpendicular coupling between adjacent FM layers is obtained by introducing an interlayer thickness fluctuation. Recently, Slonczewski's proximity magnetism model has been used to explain the 90° interlayer exchange coupling found in several FM/AF/FM multilayers.<sup>18-21</sup> In his paper, Slonczewski simply assumed a strong FM/AF interfacial coupling and an AF without intrinsic anisotropy.<sup>17</sup> As pointed out by van der Heijden *et al.*,<sup>19</sup> the AF magnetocrystalline anisotropy should be taken into account, especially for NiO in oxide-based Fe<sub>3</sub>O<sub>4</sub>/NiO/Fe<sub>3</sub>O<sub>4</sub> trilayers. In this article, we will extend the proximity magnetism model by including a uniaxial anisotropy of the AF and modifying the interface exchange coupling. With little change, this model can also be applied to FM/AF exchange biased bilayers. Therefore, results to complementing our previous study<sup>8</sup> on the exchange bias are presented in this paper as well.

### II. THEORETICAL MODEL

In order to clearly illustrate the role of interlayer coupling in a FM/AF/FM trilayer within the proximity magnetism model, we shall exclude the magnetostatic interlayer coupling and the Ruderman-Kittel-Kasuya-Yosida (RKKY-) like coupling. Furthermore, we shall assume that the FM moments rotate uniformly in the presence of an applied field. This can be achieved experimentally by choosing a FM layer, which is much thinner than its magnetic coherent length but thick enough so that it does not break into multidomains. Figure 1 shows the magnetic moment configuration for a FM/AF/FM trilayer film that lies in the  $x$ - $y$  plane. The

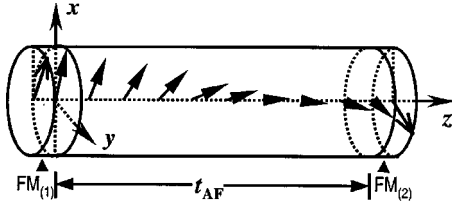


FIG. 1. Schematic representation of the helical structure of AF moments with both ends exchange-coupled to ferromagnets. To simplify picture, only one sublattice of the AF, with which both the FM layers are coupled, is shown. The angles are indicated in text.

arrow at each end represents the magnetization  $\mathbf{M}_{\text{FM}(i)}$  ( $i = 1$  and  $2$ ) for each FM layer, which rotates away from the AF easy axis, the  $x$  axis, by an angle of  $\alpha_{(i)}$ . The series of arrows inside the AF represent the moments of one sublattice. Due to the interface exchange coupling, a twisting of the AF moments along the thickness direction is expected if the two FM magnetizations are not parallel. Thus the energy including the volume energy of the AF layer and the interfacial exchange coupling energies can be written in a continuum form as

$$E_{SW} = \int_0^{t_{\text{AF}}} \left[ A_{\text{AF}} \left( \frac{d\varphi}{dz} \right)^2 + K_{\text{AF}} \sin^2 \varphi \right] dz - J_{E(1)} \times \cos(\varphi - \alpha_{(1)}) \Big|_{z=0} - J_{E(2)} \cos(\varphi - \alpha_{(2)}) \Big|_{z=t_{\text{AF}}}, \quad (1)$$

where  $A_{\text{AF}}$  and  $K_{\text{AF}}$  are exchange coupling constant and uniaxial anisotropy constant of the AF layer with finite thickness  $t_{\text{AF}}$ , respectively. The moments of the AF layer at the interface are exchange coupled with the FM layers by exchange coupling constants of  $J_{E(i)}$ . Without losing generality, we assume that the interface exchange couplings are ferromagnetic, i.e.,  $J_{E(i)} > 0$ , and that the direction and motion of the FM and AF moments is confined to the film plane. The spatial variation of the moment orientation inside the AF layer is characterized by the angle  $\varphi(z)$  with respect to the  $x$  axis. Using the variational method to minimize the total energy, the AF moment structure is given by the differential equation for  $\varphi(z)$ :

$$2A_{\text{AF}} \left( \frac{d^2\varphi}{dz^2} \right) - K_{\text{AF}} \sin(2\varphi) = 0, \quad (2)$$

with the boundary conditions

$$\left. \left( \frac{d\varphi}{dz} \right) \right|_{z=0} = \frac{J_{E(1)}}{2A_{\text{AF}}} \sin(\varphi - \alpha_{(1)}),$$

$$\left. \left( \frac{d\varphi}{dz} \right) \right|_{z=t_{\text{AF}}} = \frac{J_{E(2)}}{2A_{\text{AF}}} \sin(\varphi - \alpha_{(2)}). \quad (3)$$

The variational method has been used to describe the in-plane domain structure<sup>22</sup> and magnetization reversal<sup>23</sup> of ultrathin FM thin films. Two-dimensional domain patterns of the FM films have been obtained as solutions to the imaginary time sine-Gordon equation.<sup>22</sup> Equation (2), while similar, describes the configuration of the AF moment orienta-

tion, which is uniform in the film plane but varies in the thickness direction. The total energy of a FM/AF/FM trilayer should include the magnetocrystalline anisotropy energies of the FM layers. However, the general behavior we wish to study is not significantly influenced by the anisotropy so we shall ignore it. In addition, we shall assume that the magnetization  $\mathbf{M}_{\text{FM}(1)}$  of the pinned FM layer is always kept along the  $x$  axis, i.e.,  $\alpha_{(1)} = 0^\circ$  [note that  $\varphi(z=0)$  is not forced to be zero], and the other  $\mathbf{M}_{\text{FM}(2)}$  is free to rotate ( $\alpha_{(2)}$  is denoted by  $\alpha$  in the following). Thus the FM layer, FM(1) is considered to be pinned or a magnetically hard layer having the same easy axis as the AF while the layer FM(2) is magnetically soft. We will demonstrate that even this simple model gives very interesting and complex interlayer coupling and magnetization behavior that explains some experimental observations in FM/AF/FM trilayer or multilayer films.

Equation (2) cannot be solved analytically with the given boundary conditions, which determine the behavior of the AF moments as we will show in Sec. III. Therefore we have performed numerical calculations by transforming Eqs. (2) and (3) into a discrete form with step size of  $10^{-3} \delta_w$ , where  $\delta_w = \sqrt{A_{\text{AF}}/K_{\text{AF}}}$ . Our results are independent of step size in this regime. In the following, we present our numerical results for the AF thickness normalized by the characteristic domain wall length  $\delta_w$  and the energy  $E_{SW}$  and interfacial coupling constants normalized by the domain wall energy parameter  $\sigma_w = 2\sqrt{A_{\text{AF}}K_{\text{AF}}}$ . Note that for a  $180^\circ$  domain wall the wall energy is  $2\sigma_w$  and the wall width  $\pi\delta_w$ .

Since most reports of the perpendicular interlayer coupling were based on hysteresis loop measurements, in which the FM magnetization is reversed, we have computed the total energy of the trilayer with the FM magnetization  $\mathbf{M}_{\text{FM}(2)}$ , rotating over  $180^\circ$ . In the following section, we will first present the magnetization behavior of a trilayer with perfect FM/AF interfaces so that the AF moments of one sublattice are coupled with both the FM magnetizations at the interfaces. Then we will discuss the possibility of perpendicular interlayer coupling by introducing fluctuations at the interfaces and considering the granularity of the AF.

### III. RESULTS AND DISCUSSION

In our previous study<sup>8</sup> of FM/AF bilayers, the exchange bias was dependent on the AF thickness and the interfacial exchange coupling compared with  $\delta_w$  and  $\sigma_w$ , respectively. If the interfacial exchange coupling is large enough, e.g., with a value greater than the AF domain wall energy  $\sigma_w$ , an irreversible transition of the AF moments occurs during the rotating of the FM magnetization, resulting in an enhanced coercivity of the FM but no exchange bias. This implies that when exchange bias is experimentally observed in FM/AF bilayers the interfacial coupling must be smaller than  $\sigma_w$ . The interfacial coupling strength may vary with the interface morphology. We shall assume two interfacial exchange couplings  $J_{E(1)}$  and  $J_{E(2)}$ , which may take on different values relative to  $\sigma_w$ , and are not necessarily equal to each other. The numerical results will fall into two categories: (1)  $J_{E(1)} \leq \sigma_w$  and (2)  $J_{E(1)} > \sigma_w$ .

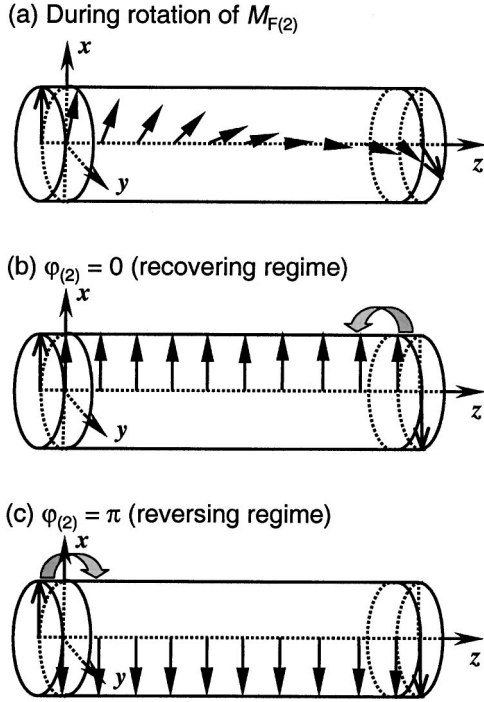


FIG. 2. Schematic representations of the AF moment configurations in response to the rotation of the FM magnetization  $\mathbf{M}_{FM(2)}$ : (a) a would-up helical structure forms while the FM magnetization rotates away from the AF easy axis; (b) in the ‘‘recovering’’ regime, as  $\mathbf{M}_{FM(2)}$  approaches  $180^\circ$ , the AF moments rotate backward to recover their initial orientation; and (c) in the ‘‘reversing’’ regime, the AF moment structure springs forward and the moments have a  $180^\circ$  orientation. The curved arrows show the directions of the AF moment motions.

### A. $J_{E(1)} \leq \sigma_w$

Figure 2 illustrates the orientation and motion of the AF moments with  $\mathbf{M}_{FM(1)}$  fixed and  $\mathbf{M}_{FM(2)}$  rotating away from the  $x$  axis. The angles that the AF moments at interfaces make with FM(1) and FM(2) are denoted by  $\varphi_{(1)}$  and  $\varphi_{(2)}$ , respectively. First let us consider the case of  $J_{E(1)} = 0.4 \sigma_w$ ,  $J_{E(2)} = 0.6 \sigma_w$ , and  $t_{AF} = 1.0 \delta_w$ . As  $\mathbf{M}_{FM(2)}$  rotates away from the easy axis, the AF moment structure twists as shown in Fig. 2(a). This helical structure develops further as the AF moments at the AF/FM(2) interface try to follow the rotating  $\mathbf{M}_{FM(2)}$ . The total energy  $E_{SW}$  of the FM/AF/FM trilayer, the volume energy  $E_{vol}$  given by the integral in Eq. (1), and the interface angles  $\varphi_{(1)}$  and  $\varphi_{(2)}$  of the AF layer are shown in Fig. 3. The AF moments at interface always lag behind the magnetization  $\mathbf{M}_{FM(2)}$  as it rotates with the difference between  $\alpha$  and  $\varphi_{(2)}$  increasing with increasing  $\alpha$ . When this the difference becomes  $90^\circ$ , further winding of the AF generates exchange and anisotropy energies that can not be sustained by the interfacial couplings. At this point, the AF moments rotate back and return to their original positions while  $\mathbf{M}_{FM(2)}$  continues to rotate to the opposite direction, i.e.,  $\alpha = 180^\circ$  [see Fig. 2(b)]. We call this kind of AF moment motion the ‘‘recovering regime.’’

For larger values of  $J_{E(2)}$ , the AF moment motion is different. Figure 4 shows the resulting numerical calculation for the case that  $J_{E(1)}$  and  $t_{AF}$  are the same as that of the previous case but  $J_{E(2)} = 0.8 \sigma_w$ . When the AF moments at the

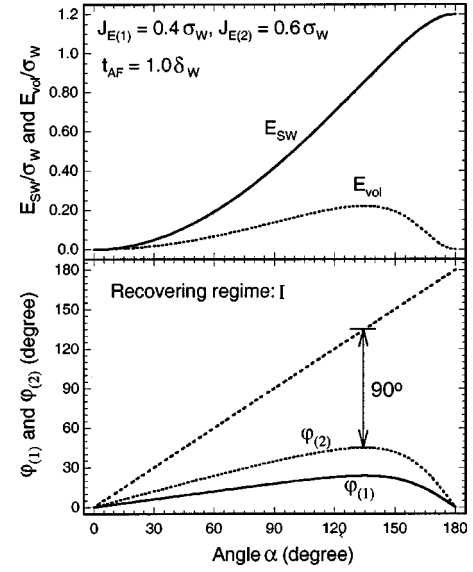


FIG. 3. Total energy  $E_{SW}$  of the FM/AF/FM trilayer and the angles  $\varphi_{(1)}$  and  $\varphi_{(2)}$  that the AF moments make with respect to the AF easy axis at the two interfaces in the case of  $J_{E(1)} = 0.4 \sigma_w$ ,  $J_{E(2)} = 0.6 \sigma_w$ , and  $t_{AF} = 1.0 \delta_w$ . The volume energy  $E_{vol}$  of the AF layer is also shown by a dotted line. The straight line in the bottom figure indicates the angle  $\alpha$  of the FM for comparison.

AF/FM(2) interface reach or pass through the AF hard axis we find that the helical structure becomes unstable when  $\alpha$  reaches a critical value  $\alpha_{cri}$  (about  $140^\circ$  in this case). The helical structure of the AF moments ‘‘springs’’ forward, settling down in a new stable state that still contains some twist. Eventually, as  $\mathbf{M}_{FM(2)}$  has completed its rotation to the opposite direction, the AF structure has also rotated by  $180^\circ$  as shown in Fig. 2(c). When  $\mathbf{M}_{FM(2)}$  rotates from  $180^\circ$  back to  $0^\circ$ , another discontinuous jump of the AF moments occurs at a critical angle of  $117^\circ$ . In this ‘‘reversing regime,’’ the mo-

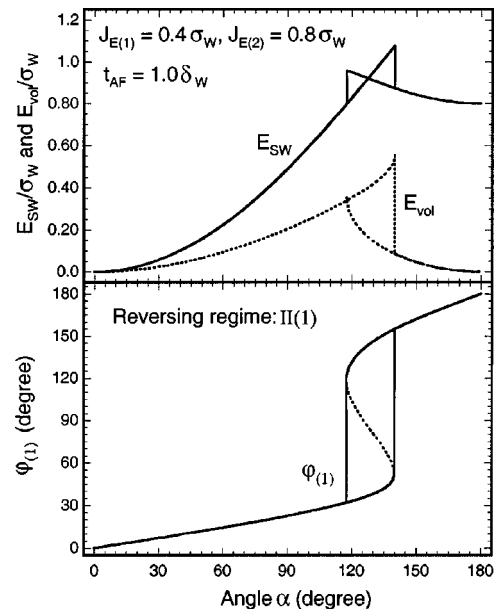


FIG. 4. Total energy  $E_{SW}$ , AF volume energy  $E_{vol}$ , and the angle  $\varphi_{(1)}$  during the rotation of  $\mathbf{M}_{FM(2)}$  in the case of  $J_{E(1)} = 0.4 \sigma_w$ ,  $J_{E(2)} = 0.8 \sigma_w$ , and  $t_{AF} = 1.0 \delta_w$ . The dotted line segment of  $\varphi_{(1)}$  indicates a metastable state for the AF.

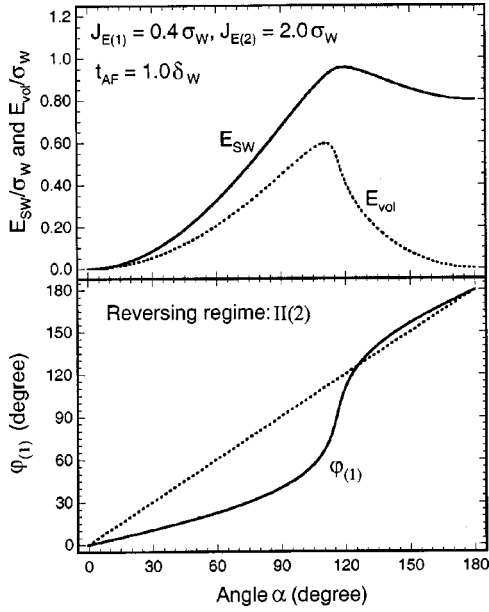


FIG. 5. Total energy  $E_{SW}$ , AF volume energy  $E_{vol}$ , and the angle  $\varphi_{(1)}$  during the rotation of  $\mathbf{M}_{FM(2)}$  in the case of  $J_{E(1)} = 0.4 \sigma_W$ ,  $J_{E(2)} = 2.0 \sigma_W$ , and  $t_{AF} = 1.0 \delta_W$ . The straight line in the bottom figure indicates the angle  $\alpha$  for comparison.

tion of the AF moments is irreversible since at the transition the total energy of the trilayer is discontinuous and the parallel ( $\alpha = 0^\circ$ ) and antiparallel alignments ( $\alpha = 180^\circ$ ) of the two ferromagnetic magnetizations are stable states with a minimized energy.

In exchange biased bilayers, the energy difference at the transition accounts for the hysteresis energy loss,<sup>8,9</sup> which has been experimentally observed.<sup>4,5</sup> Soeya *et al.*<sup>24</sup> have systematically investigated this effect based on the coherent rotation model of Jacobs and Bean.<sup>25</sup> This rotational hysteresis was also found by in-plane magnetic torque measurements in epitaxial Co/Mn multilayers, and was attributed to the irreversible motion of the magnetic moments in the Mn layers with respect to the rotating Co magnetization.<sup>26</sup> In addition, the authors suggested that interlayer exchange coupling between successive Co layers would not develop unless the Mn moments were antiferromagnetically ordered.

It is possible to have a reversible transition within the reversing regime. As shown in Fig. 5 for the case of a larger  $J_{E(2)}$  in comparison with those in the previous cases, the AF moments, represented by  $\varphi_{(1)}$ , rotate smoothly with the magnetization  $\mathbf{M}_{FM(2)}$ . At first the AF moments lag behind  $\mathbf{M}_{FM(2)}$ . Then the angle  $\varphi_{(1)}$  increases rapidly when  $\alpha$  is around  $110^\circ$ . We can see that  $\varphi_{(1)}$  crosses over the straight line indicating the value of  $\alpha$  at  $\alpha = 124^\circ$ . This means that the helical structure of the AF moments gradually “swing” forward from a position lagging behind  $\mathbf{M}_{FM(2)}$  to one in advance of it. No hysteresis is found in this case.

Based on these results we can construct magnetic phase diagrams in terms of the AF thickness  $t_{AF}$  and the interfacial exchange coupling  $J_{E(2)}$  for different  $J_{E(1)}$  shown in Fig. 6. Figure 6(a) corresponds to the exchange bias in FM/AF bilayers that we have investigated based on an extended planar domain wall model.<sup>8</sup> Phase I represents the recovering

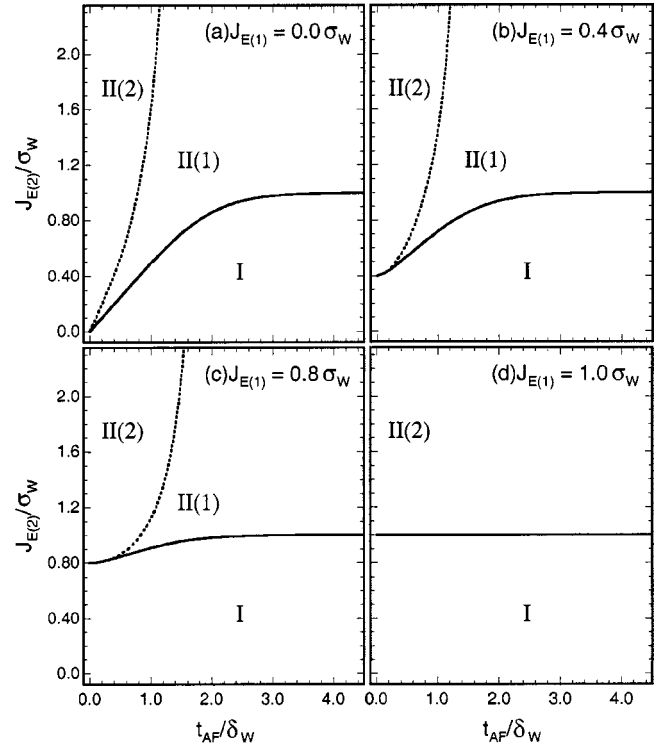


FIG. 6. Magnetic phase diagrams for a FM/AF/FM trilayer with smooth interfaces for (a)  $J_{E(1)} = 0.0 \sigma_W$ , (b)  $J_{E(1)} = 0.4 \sigma_W$ , (c)  $J_{E(1)} = 0.8 \sigma_W$ , and (d)  $J_{E(1)} = 1.0 \sigma_W$ . The solid line separates the “recovering” region I from the “reversing” region II. The dotted line separates the irreversible region II(1) from the reversible region II(2). The results shown in (a)  $J_{E(1)} = 0$  apply to the exchange coupled FM/AF bilayers.

regime. The reversing regime is separated into two phases II(1) and II(2), depending upon whether or not the AF moments show an irreversible behavior during the magnetization reversal.

Let us consider this phase diagram for exchange-coupled FM/AF bilayers in more detail. Exchange bias is obtained only in the recovering regime and a coercivity appears only in the reversing regime due to the reversal of the AF moments.<sup>8</sup> We can see in Fig. 6(a) that the critical value of the interfacial exchange coupling  $J_{E(2)}^{crit(1)}$ , which separates these two regimes, is very close to but a little smaller than  $\sigma_W$  for thick AF layer. This critical interfacial coupling decreases to zero almost linearly with decreasing AF thickness when  $t_{AF}$  is smaller than  $\pi \delta_W / 2$ , i.e., half the value of a  $180^\circ$  domain wall width. As the AF thickness approaches to zero, the critical interfacial coupling becomes

$$\lim_{t_{AF} \rightarrow 0} J_{E(2)}^{crit(1)} = K_{AF} t_{AF}. \quad (4)$$

The exchange coupling  $A_{AF}$  of the bulk AF moments is not involved in this formula. Therefore, in the thin-AF-layer region, our calculations are consistent with those of the coherent rotation model,<sup>4,25</sup> in which a rigid rotation of the AF moments is assumed and the condition of  $J_E \leq K_{AF} t_{AF}$  is satisfied for observing exchange anisotropy.

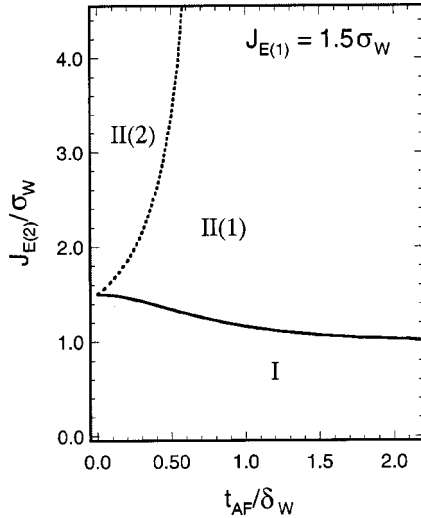


FIG. 7. Magnetic phase diagram for a FM/AF/FM trilayer with smooth interfaces with  $J_{E(1)} = 1.5 \sigma_W$ .

In the reversing regime, another characteristic value of the interfacial exchange coupling  $J_{E(2)}$  divides the reversal behavior of the AF moments into two groups. Phase II(1) is with irreversible transitions and the other, phase II(2), without. For FM/AF bilayers, the rotational hysteresis energy loss can only be obtained in phase II(1) where the irreversible transition is accompanied by an energy discontinuity. Fujiwara *et al.*<sup>27</sup> found the following formula for the second critical interfacial exchange coupling,  $J_{E(2)}^{\text{crit}(2)}$ ,

$$J_{E(2)}^{\text{crit}(2)} = \sigma_W \tan\left(\frac{t_{AF}}{\delta_W}\right). \quad (5)$$

This expression suggests that phase II(2) cannot exist in the bilayer with an AF layer thicker than  $\pi\delta_W/2$ . Our calculations for FM/AF/FM trilayers show that this critical thickness increases with increasing interfacial exchange coupling  $J_{E(1)}$ , indicating an expansion of phase II(2). For  $J_{E(1)} = 0.2, 0.4, 0.6,$  and  $0.8 \sigma_W$ , the critical thickness is 1.586, 1.639, 1.750, and 1.995  $\delta_W$ , respectively. For the case that  $J_{E(1)}$  is equal to  $\sigma_W$ , phase II(1) totally disappears from the diagram with a straight line at  $\sigma_W$  separating the reversing regime from the recovering regime.

### B. $J_{E(1)} > \sigma_W$

The motion of the AF moments can still be classified into the recovering and reversing regimes for the case of  $J_{E(1)} > \sigma_W$ . Figure 7 shows a representative magnetic phase diagram when  $J_{E(1)} = 1.5 \sigma_W$ . However, the AF moments display some different behavior during the FM magnetization reversal from those we have discussed earlier.

In the cases of  $J_{E(1)} \leq \sigma_W$ , the configuration and motion of the AF moments can be completely determined within the rotating region of the FM magnetization from  $0^\circ$  to  $180^\circ$ . Whether the AF moment motion is recoverable or reversible, all the AF moments are aligned collinearly along the AF easy axis when  $\mathbf{M}_{FM(2)}$  completes the  $180^\circ$  rotation. There is no variation of the moment arrangement inside the AF layer,

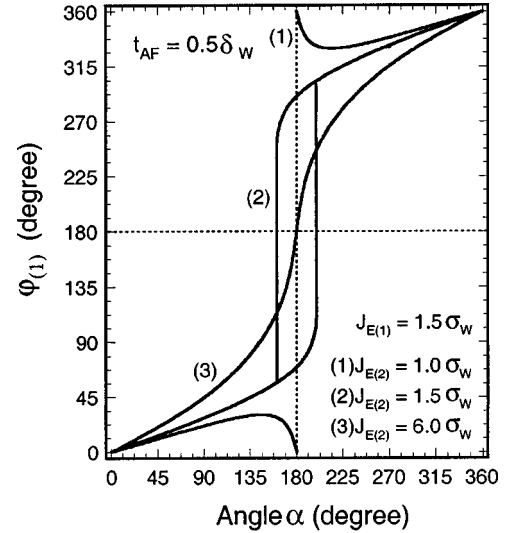


FIG. 8. Angle  $\varphi_{(1)}$  during the rotation of  $\mathbf{M}_{FM(2)}$  for a FM/AF/FM trilayer with  $J_{E(1)} = 1.5 \sigma_W$  and  $t_{AF} = 0.5 \delta_W$  in the case of (1)  $J_{E(2)} = 1.0 \sigma_W$ , in the ‘‘recovering’’ regime, (2)  $J_{E(2)} = 1.5 \sigma_W$ , in the irreversible ‘‘reversing’’ regime, and (3)  $J_{E(2)} = 6.0 \sigma_W$ , in the reversible ‘‘reversing’’ regime.

but the AF moments at the interface are forced into a ‘‘frustrated’’ state with respect to the FM magnetizations [see Figs. 2(b) and 2(c)].

Figure 8 shows three typical behaviors of the AF moments when the FM magnetization  $\mathbf{M}_{FM(2)}$  rotates over  $360^\circ$  and back to its initial position in the case of  $J_{E(1)} = 1.5 \sigma_W$ . In the recovering regime, the AF moments rotate back to their initial positions when  $\mathbf{M}_{FM(2)}$  rotates  $180^\circ$  to the opposite direction. In the reversible reversing regime, the AF moments are ‘‘dragged’’ by  $\mathbf{M}_{FM(2)}$  in rotation since their motion always lags behind  $\mathbf{M}_{FM(2)}$ . In the irreversible reversing regime, the transition does not occur until the magnetization  $\mathbf{M}_{FM(2)}$  rotates over  $180^\circ$ . In this situation, if the two FM magnetizations are oriented antiparallel, we can have two AF structures wound up in opposite direction between the FM layers.

If the interfacial exchange couplings and the AF thickness are larger, the situation is more complicated. A series of AF helical structures that twist over  $180^\circ$  or greater can be stabilized in the FM/AF/FM trilayer. Twisting means higher energy. Realistically, only the least-twisted structure corresponding to the ground state exists in the trilayer, in the presence of an external-field and thermal perturbation.

### C. Extended proximity magnetism

The above discussion is based on the assumptions that the interfacial coupling is ferromagnetic and the FM magnetizations ‘‘see’’ the same AF sublattice. With these assumptions the FM magnetizations prefer a parallel alignment. If the  $\mathbf{M}_{FM(1)}$  and  $\mathbf{M}_{FM(2)}$  ‘‘see’’ different sublattices, the ferromagnetic interfacial couplings result in an antiparallel alignment of the FM magnetizations. Slonczewski<sup>16</sup> reasoned that interface roughness would result in a thickness fluctuation of the AF spacer and thereby produce a competition between the parallel and antiparallel alignments of the FM magnetizations. Then the compromising solution is to create a noncollinear

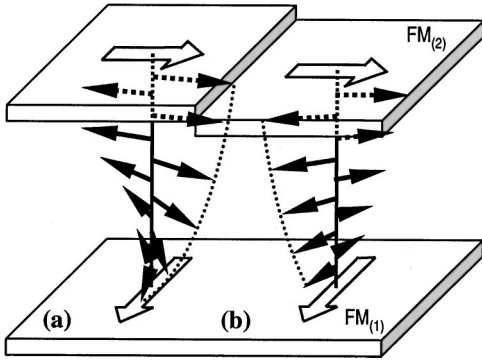


FIG. 9. Two AF moment configurations between two ferromagnetic layers with the magnetization orientations perpendicular to each other, in which the AF interlayer differs by a monatomic step.

coupling between the magnetizations with the AF moments twisting along the thickness direction (see Fig. 9). Assuming strong interfacial exchange couplings and no in-plane magnetocrystalline anisotropy for the AF, the mean coupling energy  $W_S$  can be written as the following quadratic form:<sup>17</sup>

$$W_S = C_+(\alpha)^2 + C_-(\alpha - \pi)^2. \quad (6)$$

The contributions of parallel and antiparallel coupling are represented by  $C_+$  and  $C_-$ , respectively. For  $C_+ = C_-$ , minimizing the mean coupling energy gives the favored configuration with the FM magnetizations aligned perpendicularly. Because the energy is increased by the twist in the moment direction, it turns out that the perpendicular coupling strength is proportional to the inverse of the AF thickness.<sup>17,28</sup>

Before discussing our extension to Slonczewski's "proximity coupling" in FM/AF/FM trilayers by incorporating arbitrary interfacial coupling and anisotropy, let us consider the problem on the interfacial coupling with the AF interlayer. For a perfectly smooth and totally uncompensated interface, the interfacial exchange coupling would be orders of magnitude larger than the AF domain wall energy.<sup>4</sup> In reality, a totally uncompensated surface becomes partially compensated due to interface roughness. By studying the exchange anisotropy in  $\text{Ni}_{81}\text{Fe}_{19}/\text{CoO}$  bilayers, Takano *et al.*<sup>29</sup> proposed a model, in which only the interfacial uncompensated AF moments contribute to the interfacial coupling, resulting in the exchange anisotropy with a magnitude consistent with the experimental observations. Similarly, even a totally compensated interface because partially uncompensated with roughness. Malozemoff<sup>30</sup> developed a random field theory for bilayers with compensated interfaces and demonstrated a nonzero interfacial exchange energy, whose magnitude is also by orders of magnitude less than that of a fully uncompensated interface.<sup>30</sup>

The AF layer can be polycrystalline or single-crystal depending upon the film growth method. For trilayers with a polycrystalline AF layer, any AF moment twisting is confined in each grain, and the coherent length is determined by the grain size, assuming that there is no coupling among grains.<sup>31</sup> For single-crystal antiferromagnets, due to the interface roughness, the AF interlayer consists of a multidomain state as a result of Malozemoff's random field

mechanism.<sup>30</sup> We therefore assume that the trilayer with interface roughness can be described by Eq. (6) but with energies given by Eq. (1), i.e.,

$$W_S = c_+ E_{SW}(\alpha) + c_- E_{SW}(\alpha - \pi). \quad (7)$$

Here,  $c_+$  and  $c_-$  are dimensionless factors with  $c_+ + c_- = 1$ .

In the limit of no magnetocrystalline anisotropy for the AF, the twisting inside the AF can be described by  $\varphi(z) = \varphi_{(1)} + az$ , which is explicitly a solution of Eq. (2). This relationship can be simplified to be  $\varphi(z) = (z/t_{AF})\alpha$  for strong interfacial couplings as discussed in Slonczewski's paper,<sup>17</sup> and then the total energy of the trilayer is quantitatively equal to the twisting energy of the AF. Expression (6) is viable in this case.

As previously explained, the interfacial exchange coupling is reduced by orders of magnitude due to the FM/AF interface morphology. The following discussion will focus on the interesting situation in which the interfacial coupling  $J_{E(i)}$  is comparable to the AF domain wall energy  $\sigma_W$ .<sup>32</sup>

A thick AF interlayer allows large twisting. If the AF thickness is larger than  $\pi\delta_W/2$ , the energy of the trilayer is then related to the FM magnetization rotation angle  $\alpha$  by a cosine form rather than a quadratic one. However, a  $90^\circ$  coupling can still be obtained in a trilayer by balancing AF moment twistings, i.e.,  $c_+ = c_-$ . However, we must consider the continuity of the coupling among the AF moments throughout the thickness, especially for a granular AF interlayer.<sup>33</sup> Furthermore, most of the cited experimental results<sup>18-20</sup> were obtained in samples with the AF interlayer thickness around several nanometers. In bulk NiO, the domain wall width for the moments rotating out of the easy plane was about 11 nm.<sup>34</sup> It is known that the anisotropy of a thin film differ from and, is generally less than, that of the bulk material. As a result, the domain wall width of an AF thin film should be larger. Mauri *et al.*<sup>35</sup> have estimated the domain wall width of  $\text{Fe}_{50}\text{Mn}_{50}$  to be 54 nm, which is a typical order of magnitude for pure metallic materials and alloys. Therefore, it is more relevant to consider the case when  $t_{AF}$ , the effective AF thickness, is smaller than  $\delta_W$ .

In the case of small AF interlayer thickness, the AF moments rotate almost coherently with the FM magnetization, i.e.,  $\varphi(z) \approx \varphi_{(1)}$ . So, the total energy includes only the interfacial coupling and the AF magnetocrystalline anisotropy. To study the proximity magnetism, we first assume that  $c_+ = c_-$  for convenience. According to the calculations presented in the previous section, the AF moments will display recovering, irreversible and reversible reversing behaviors during the FM magnetization reversal depending upon the interfacial couplings and the AF thickness. In the recovering regime, the FM magnetizations always prefer a perpendicular coupling since the corresponding energy is the lowest. The coupling strength decreases with increasing  $t_{AF}$  but it is not a  $1/t_{AF}$  dependence.

In the reversing regime, the  $90^\circ$  interlayer coupling is not always energetically favored. Figure 10 shows the dependence of the mean coupling energy  $W_S$  on the  $\mathbf{M}_{\text{FM}(2)}$  angle  $\alpha$  in several cases with the interfacial coupling  $J_{E(1)} = 0.4\sigma_W$ . For a trilayer with an AF thickness  $t_{AF} = 1.0\delta_W$ , we see that the perpendicular coupling and the

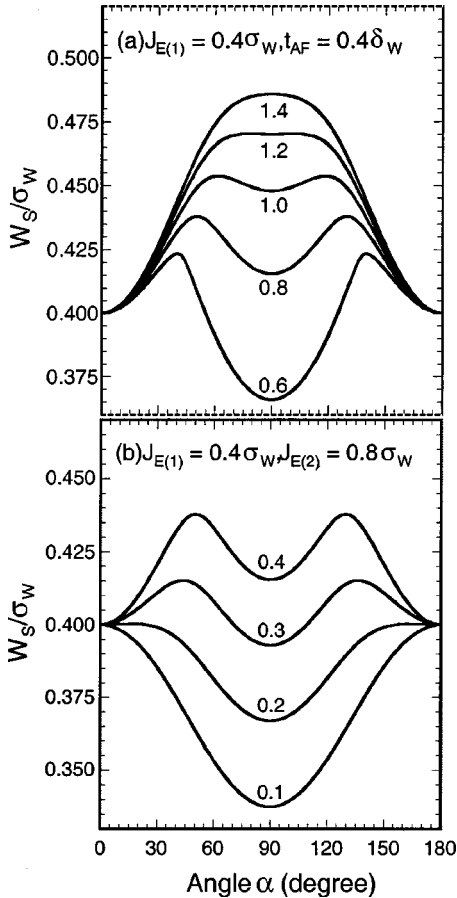


FIG. 10. Slonczewski's mean coupling energy  $W_S$  for trilayers with (a)  $J_{E(1)} = 0.4 \sigma_W$  and  $t_{AF} = 0.4 \delta_W$ . The numbers associated with the curves are values of the interfacial exchange coupling  $J_{E(2)}$  normalized by  $\sigma_W$ . (b)  $J_{E(1)} = 0.4 \sigma_W$  and  $J_{E(2)} = 0.8 \sigma_W$ . The numbers associated with the curves are values of the AF thickness  $t_{AF}$  normalized by  $\delta_W$ .

collinear (parallel and antiparallel) coupling are stable states as  $J_{E(2)}$  is relatively small [see Fig. 10(a)]. The mean coupling energy for perpendicular coupling is lower than that for collinear coupling when  $J_{E(2)} = 0.6 \sigma_W$ , but higher than that when  $J_{E(2)} = 0.8 \sigma_W$  or larger. With even larger  $J_{E(2)}$ , e.g.,  $J_{E(2)} = 1.4 \sigma_W$ , the perpendicular coupling is no longer stable. Figure 10(b) illustrates the change of the mean coupling energy with the AF thickness. The  $\alpha$ -dependent mean coupling energy cannot be fit either with the formula  $E_c = -A_{12} \cos \alpha + 2B_{12} \cos^2 \alpha$ , for bilinear and biquadratic interlayer couplings or with Slonczewski's Eq. (6). We must consider the energy difference between the perpendicular coupling and collinear coupling to see the coupling preference of the FM magnetizations. Results are shown in Fig. 11. In the trilayer of a thin AF, the perpendicular interlayer is favored and the mean coupling energy increases with increasing AF thickness. From this figure, we see that the energy difference decreases with the AF thickness, suggesting the perpendicular coupling strength also decreases. For some cases, represented by the solid curve in Fig. 11, at a certain AF thickness the energy difference vanishes and the FM coupling cross over into a collinear configuration. This kind of transition from perpendicular interlayer coupling to collinear coupling with increasing AF thickness has been found by

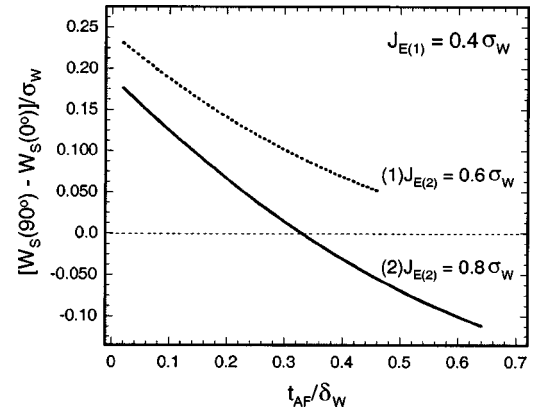


FIG. 11. Difference between the mean coupling energies with the two FM magnetizations aligned perpendicularly and collinearly.

van Heijden *et al.* in  $\text{Fe}_3\text{O}_4/\text{NiO}/\text{Fe}_3\text{O}_4$  trilayers when the NiO thickness was 5.4 nm.<sup>19</sup>

The decrease of the perpendicular interlayer coupling strength  $C_+$  and  $C_-$ , with increasing Mn interlayer thickness up to 2.5 nm was also found in Fe/Mn/Fe trilayers.<sup>20</sup> However, the couplings in these trilayers are more complicated than those in the oxide-based trilayers. The RKKY coupling is greatly affected by the quality of the Mn interlayers. The epitaxial growth depends sensitively on substrate, temperature, cleanliness, and growth rate.<sup>35</sup> The fact that no coupling is found in a Fe/Mn/Fe trilayer<sup>20</sup> with a Mn layer thicker than 2.5 nm may result from the failure to obtain a thicker Mn layer than the 25 Mn monolayers required for a pure bct Mn phase, as discussed by Purcell *et al.*<sup>36</sup>

In our previous study, the exchange anisotropy in FM/AF bilayers can not exceed the AF domain wall energy.<sup>8</sup> Similarly, in FM/AF/FM trilayers, no matter whether the interlayer coupling is perpendicular or collinear, the coupling strength is relatively small compared with the AF domain wall energy. Usually the domain wall energies of AF materials are around 10 ergs/cm<sup>2</sup>. So, our calculations are quantitatively consistent with the experimental observations that find the perpendicular interlayer coupling in the range of several ergs/cm<sup>2</sup>.<sup>18-20</sup>

#### IV. SUMMARY

In this work, we have studied the interlayer exchange coupling in FM/AF/FM trilayers. Starting from the differential equations describing a twisting of the FM moments throughout the thickness direction and couplings with the FM magnetizations at the FM/AF interfaces, we can explain the behaviors of the AF moments during the process of the FM magnetization reversal. Standing at Slonczewski's view of the proximity magnetism, the study of interlayer coupling of the adjacent FM layers negotiated by the AF layer can therefore be completed within the model by including the AF magnetocrystalline anisotropy. Numerical calculations show that the perpendicular interlayer coupling is obtained under certain conditions, depending upon the interfacial coupling and the AF thickness. In all cases, the coupling strength is limited by the AF domain wall energy  $\sigma_W$ .

Although our results give a clear illustration of a magnetic proximity effect in FM/AF/FM trilayers, two concerns about

the model are left for further study. One has to do with knowing the relative orientations of the FM magnetizations with respect to the AF anisotropy direction. For single crystal films, in-plane lattice matches among the layers determine the relationship if the magnetocrystalline anisotropy is taken into account. For granular trilayers, the in-plane anisotropy axis of AF grains is likely to have a distribution, leading to an averaging. The other concern is the possibility of “spin flop coupling,” which was experimentally observed in some exchange-coupling FM/AF bilayers and multilayers.<sup>5,12</sup> This

means that the FM magnetizations tend to be perpendicular to the AF moments, especially in films with compensated interfaces. Clarifying the perpendicular interlayer coupling in these two cases requires more detailed study.

#### ACKNOWLEDGMENTS

This work was supported by the National Science Foundation under Grant No. ECD-8907068.

- <sup>1</sup>M. N. Baibich, J. M. Broto, A. Fert, F. Neuyen Van Dau, F. Petroff, P. Eitenne, G. Creuzet, A. Friederich, and J. Chazelas, *Phys. Rev. Lett.* **61**, 2472 (1988).
- <sup>2</sup>For a review article on GMR applications, see M. Daughton, *J. Magn. Magn. Mater.* **192**, 334 (1999).
- <sup>3</sup>D. Heim, R. Fontana, C. Tsang, V. Speriosu, B. Gurney, and M. Williams, *IEEE Trans. Magn.* **30**, 316 (1994); C. Tsang, R. E. Fontana, Jr., T. Lin, D. E. Heim, V. S. Speriosu, B. A. Gurney, and M. L. Williams, **30**, 3801 (1994).
- <sup>4</sup>W. H. Meiklejohn and C. P. Bean, *Phys. Rev.* **102**, 1413 (1956); **105**, 904 (1957); W. H. Meiklejohn, *J. Appl. Phys.* **33**, 1328 (1962).
- <sup>5</sup>For recent review articles, see J. Nogués and I. K. Schuller, *J. Magn. Magn. Mater.* **192**, 203 (1999); A. E. Berkowitz and K. Takano, *ibid.* **200**, 552 (1999).
- <sup>6</sup>L. Néel, in *Selected Works of Louis Néel*, edited by N. Kurti (Gordon and Breach, New York, 1988), p. 469.
- <sup>7</sup>C. Mauri, H. C. Siegmann, P. S. Bagus, and E. Kay, *J. Appl. Phys.* **62**, 3047 (1987).
- <sup>8</sup>H. Xi and R. M. White, *Phys. Rev. B* **61**, 80 (2000).
- <sup>9</sup>C. Schlenker, *J. Phys. (Paris), Colloq.* **2**, 157 (1968).
- <sup>10</sup>H. Xi, R. M. White, and S. M. Rezende, *Phys. Rev. B* **60**, 14 837 (1999); *J. Appl. Phys.* **87**, 4960 (2000).
- <sup>11</sup>H. Xi and R. M. White, *IEEE Trans. Magn.* (to be published).
- <sup>12</sup>For example, Y. Ijiri, J. A. Borchers, R. W. Erwin, S.-H. Lee, P. J. van der Zaag, and R. M. Wolf, *Phys. Rev. Lett.* **80**, 608 (1998).
- <sup>13</sup>N. Koon, *Phys. Rev. Lett.* **78**, 4865 (1997).
- <sup>14</sup>T. C. Schulthess and W. H. Butler, *Phys. Rev. Lett.* **81**, 4516 (1998); *J. Appl. Phys.* **85**, 5510 (1999).
- <sup>15</sup>For review articles, see B. Heinrich and J. F. Cochran, *Adv. Phys.* **42**, 523 (1993); K. B. Hathaway, in *Ultrathin Magnetic Structures II*, edited by B. Heinrich and J. A. C. Bland (Springer-Verlag, Berlin, 1994), p. 45.
- <sup>16</sup>J. C. Slonczewski, *Phys. Rev. Lett.* **67**, 3172 (1991).
- <sup>17</sup>J. C. Slonczewski, *J. Magn. Magn. Mater.* **150**, 13 (1995).
- <sup>18</sup>M. E. Filipkowski, J. J. Krebs, G. A. Prinz, and C. J. Gutierrez, *Phys. Rev. Lett.* **75**, 1847 (1995).
- <sup>19</sup>P. A. A. van der Heijden, C. H. W. Swüste, W. J. M. de Jonge, J. M. Gaines, J. T. W. M. van Eemeren, and K. M. Schep, *Phys. Rev. Lett.* **82**, 1020 (1999).
- <sup>20</sup>S.-S. Yan, R. Schreiber, F. Voges, C. Osthöver, and P. Grünberg, *Phys. Rev. B* **59**, R11 641 (1999).
- <sup>21</sup>Several experimental measurements revealed the existence of spin-density wave (SDW) in Fe/Cr multilayers, e.g., E. E. Fullerton, S. D. Bader, and J. L. Robertson, *Phys. Rev. Lett.* **77**, 1382 (1996); A. Schreyer, C. F. Majkrzak, Th. Zeidler, T. Schmitte, P. Bödeker, K. Theis-Bröhl, A. Abromeit, J. A. Dura, and T. Watanabe, *ibid.* **79**, 4914 (1997). The stability of incommensurate SDW and helical SDW that arises from the incommensuration between the hole and electron Fermi surfaces in Fe/Cr multilayers has been theoretically investigated, e.g., Z.-P. Shi and R. S. Fishman, *ibid.* **78**, 1351 (1997); R. S. Fishman, *ibid.* **81**, 4979 (1998). The discussion on this topic will not be included in this paper.
- <sup>22</sup>J. Castro, S. T. Chui, and V. N. Ryzhov, *Phys. Rev. B* **60**, 10 271 (1999); S. T. Chui and V. N. Ryzhov, *Phys. Rev. Lett.* **78**, 2224 (1997).
- <sup>23</sup>A. F. Khapikov, *Phys. Rev. Lett.* **80**, 2209 (1998).
- <sup>24</sup>S. Soeya, S. Nakamura, T. Imagawa, and S. Narishige, *J. Appl. Phys.* **77**, 5838 (1995).
- <sup>25</sup>I. S. Jacobs and C. P. Bean, in *Magnetism-III*, edited by G. T. Rado and H. Suhl (Academic, New York, 1963), p. 323.
- <sup>26</sup>Y. Henry and K. Ounadjela, *Phys. Rev. Lett.* **76**, 1944 (1996).
- <sup>27</sup>H. Fujiwara, C. Hou, M. Sun, H. S. Cho, and K. Nishioka, *IEEE Trans. Magn.* **35**, 3082 (1999).
- <sup>28</sup>A. I. Morozov and A. S. Sigov, *Phys. Solid State* **41**, 1130 (1999).
- <sup>29</sup>K. Takano, R. H. Kodama, A. E. Berkowitz, W. Cao, and G. Thomas, *Phys. Rev. Lett.* **79**, 1130 (1997); *J. Appl. Phys.* **83**, 6888 (1998).
- <sup>30</sup>A. P. Malozemoff, *Phys. Rev. B* **35**, 3679 (1987); *J. Appl. Phys.* **63**, 3874 (1988).
- <sup>31</sup>M. D. Stiles and R. D. McMichael, *Phys. Rev. B* **59**, 3722 (1999).
- <sup>32</sup>M. Rubinstein, *J. Appl. Phys.* **85**, 5880 (1999).
- <sup>33</sup>H. Xi, B. Bian, K. R. Mountfield, Z. Zhuang, D. E. Laughlin, and R. M. White (unpublished).
- <sup>34</sup>M. T. Hutching, B. D. Rainford, and H. J. Guggenheim, *J. Phys. C* **3**, 307 (1970); M. T. Hutching and E. J. Samuelsen, *Phys. Rev. B* **6**, 3447 (1972).
- <sup>35</sup>D. Mauri, E. Kay, D. Scholl, and J. K. Howard, *J. Appl. Phys.* **62**, 2929 (1987).
- <sup>36</sup>S. T. Purcell, M. T. Johnson, N. W. E. McGee, R. Coehoorn, and W. Hoving, *Phys. Rev. B* **45**, 13 064 (1992).